A New Type of μ_4-Oxo-Bridged Copper Tetramer: Synthesis, X-ray Molecular Structure, Magnetism and Spectral Properties of (μ_4-Oxo)tetrakis(μ-bromo)bis(μ-2,6-bis(morpholinomethyl)-4-methylphenolato)tetracopper(II) and (μ_4-Oxo)tetrakis(μ-benzoato)bis(μ-2,6-bis(morpholinomethyl)-4-methylphenolato)tetracopper(II)†

Stephan Teipel,‡ Klaus Griesar,§ Wolfgang Haase,§ and Bernt Krebs*,‡

Anorganisch-Chemisches Institut der Universität Münster, D-48149 Münster, Germany, and Institut für Physikalische Chemie der Technischen Hochschule Darmstadt, D-64287 Darmstadt, Germany

Received July 28, 1993®

Reaction of $CuBr_2$ or $Cu(ClO_4)_2 \cdot 6H_2O$ and sodium benzoate with the tridentate ligand 2,6-bis(morpholinomethyl)-4-methylphenol (Hbmmk) in methanol yields two copper complexes $[Cu_4OBr_4(bmmk)_2] \cdot 2MeOH$ (**1**) and $[Cu_4O(OBz)_4(bmmk)_2] \cdot H_2O$ (**2**). The compounds were characterized by single-crystal X-ray diffraction studies and are shown to contain μ_4-oxo-bridged cluster compounds of the new type $[Cu_4OX_4L_6]$. **1** crystallizes in the monoclinic space group $P2_1/c$ with $a = 12.693(2)$ Å, $b = 12.378(2)$ Å, $c = 29.293(6)$ Å, $\beta = 96.32(3)°$, $V = 4574.4$ Å^3, and $Z = 4$. Discrepancy values of $R = 0.0324$ and $R_w = 0.0309$ were obtained for 5544 independent reflections and 517 adjustable parameters. The complex has a central μ_4-bridging oxygen surrounded tetrahedrally by four copper atoms (average Cu–O distance 1.917 Å). By copper pairing two of the Cu···Cu distances (average 3.000 Å) are significantly shorter than the other four (average 3.193 Å). The four bromine ligands and the two phenoxo groups of the deprotonated bmmk$^-$ ligand are in a μ_2-bridging mode and bridge each of the Cu···Cu vectors. The structure is completed by four terminal, N-bonded morpholine groups, one of them attached to each of the copper atoms. All copper centers are in trigonal bipyramidal coordination. Crystals of **2** are also monoclinic, space group $P2_1$, with $a = 11.889(2)$ Å, $b = 20.250(4)$ Å, $c = 12.481(3)$ Å, $\beta = 95.12(2)°$, $V = 2992.8$ Å^3, and $Z = 2$. $R = 0.0874$ and $R_w = 0.0879$ for 4792 independent reflections and 776 adjustable parameters. The complex consists of a central Cu_4O tetrahedron (average Cu–O = 1.925 Å). As in **1**, copper pairing leads in **2** to two short (average 2.992 Å) and four long Cu···Cu distances (average 3.216 Å). The bromine ligands of **1** are replaced in **2** by $\mu_{1,3}$-bridging benzoate groups. The more rigid benzoate framework leads to three different coordination polyhedra around the copper atoms: octahedral for Cu(1), square planar for Cu(2), and square pyramidal for Cu(3) and Cu(4). Magnetic susceptibility measurements in the temperature range 4.2–475.4 K indicate significant antiferromagnetic coupling between the copper(II) centers of both complexes. The experimental data were fitted to a modified Heisenberg model with two coupling constants J_{12} and J_{13}. The best least-squares fit parameters were $g = 2.19$, $J_{12} = -296$ cm^{-1}, $J_{13} = -36$ cm^{-1}, and $x_P = 2.4\%$ for **1** and $g = 2.01$, $J_{12} = -175$ cm^{-1}, $J_{13} = -18$ cm^{-1}, and $x_P = 0.8\%$ for **2**. The susceptibilities calculated with this model were found to be highly insensitive to J_{13} but very sensitive to J_{12}.

Introduction

There has been a growing awareness of the involvement of cluster compounds at the active sites of biomolecules, in addition to the long-standing interest in magnetic exchange phenomena in di- and polynuclear complexes.[1] Recent publications in this area emphasize the importance of metal oxo complexes e.g. as models for the biomineralization of iron in the ferritin core.[2] Studies on Mn_4 species indicate interesting structural and electronic consequences of the introduction of chelating ligands in place of bridging and/or terminal coordinated halide ions and perturbations to the core.[3]

Since Bertrand et al. and Bock et al.[4] characterized the first tetranuclear copper(II) complex of the general formula $[Cu_4OX_{10-n}L_n]^{n-4}$, where X represents a halide ion and L a Lewis base ligand, a number of these compounds with the special formula $[Cu_4OX_6L_4]$ (X = Br, Cl) have been synthesized.[5,6] All these complexes have the same structural framework, with four copper atoms at the corners of a tetrahedron around the central μ_4-bridging oxygen and six μ-bridging halide atoms over each edge of the tetrahedron.

In 1972 Lines et al.[7] reported the unusual magnetic properties of these compounds. They quantitatively interpreted the observed maximum in the curve of μ_{eff} vs temperature in the range 40–60 K for $Cu_4OCl_6(Ph_3PO)_4$ in terms of an oribitally degenerated ground state for the copper atoms. On the contrary, a different singlet ground state was proposed for $[(CH_3)_4N]_4[Cu_4OCl_{10}]$. Here the values of μ_{eff} steadily decrease with decreasing

* To whom correspondence should be addressed.
† Dedicated to Professor Hans Bock on the occasion of his 65th birthday.
‡ Universität Münster.
§ Technische Hochschule Darmstadt.
® Abstract published in *Advance ACS Abstracts,* January 1, 1994.

(1) Fenton, D. E.; Okawa, H. *J. Chem. Soc., Dalton Trans.* **1993**, 1349–1357.
(2) Taft, K. L.; Papaefthymiou, G. C.; Lippard, S. J. *Science* **1993**, *259*, 1302–1305.
(3) (a) Wemple, M. W.; Tsai, H.-L.; Folting, K.; Hendrickson, D. N.; Christou, G. *Inorg. Chem.* **1993**, *32*, 2025–2031. (b) Wang, S.; Tsai, H.-L.; Streib, W. E.; Christou, G.; Hendrickson, D. N. *J. Chem. Soc., Chem. Commun.* **1992**, 1427–1429.
(4) (a) Bertrand, J. A.; Kelley, J. A. *J. Am. Chem. Soc.* **1966**, *88*, 4746–4747. Bertrand, J. A. *Inorg. Chem.* **1967**, *6*, 495–498. (b) Bock, H.; tom Dieck, H.; Pyttlik, H.; Schnöller, M. *Z. Anorg. Allg. Chem.* **1968**, *357*, 54–61. Kilbourn, B. T.; Dunitz, J. D. *Inorg. Chim. Acta* **1967**, *1*, 209–216.
(5) (a) Keij, F. S.; Haasnoot, J. G.; Oosterling, A. J.; Reedijk, J.; O'Conner, C. J.; Zang, J. H.; Spek, A. L. *Inorg. Chim. Acta* **1991**, *181*, 185–193. (b) Haendler, H. M. *Acta Crystallogr.* **1990**, *C46*, 2054–2057. (c) Norman, R. E.; Rose, N. J.; Stenkamp, R. E. *Acta Crystallogr.* **1989**, *C45*, 1707–1713. (d) Brownstein, S.; Han, N. F.; Gabe, E.; Leer, F. *Can. J. Chem.* **1989**, *67*, 551–554. (e) Guy, J. T., Jr.; Cooper, J. C.; Gillardi, R. D.; Flippen-Anderson, J. L.; George, C. F., Jr. *Inorg. Chem.* **1988**, *27*, 635–638. (f) Churchill, M. R.; Rotella, F. J. *Inorg. Chem.* **1979**, *18*, 853–860.
(6) Dickinson, R. C.; Helm, F. T.; Baker, W. A., Jr.; Black, T. D.; Watson, W. H., Jr. *Inorg. Chem.* **1977**, *16*, 1530–1537 and references therein.
(7) Lines, M. E.; Ginsberg, A. P.; Martin, R. L.; Sherwood, R. C. *J. Chem. Phys.* **1972**, *57*, 1–19.

0020-1669/94/1333-0456$04.50/0

temperature. Wong et al.[8] compared the magnetic properties of a wider range of Cu_4OX_6-type complexes. They proposed a model in which orbital effects are important for the magnetic exchange. However Jones et al.[9] noted that complexes in which the magnetic properties depend on orbital effects are rare, and thus some doubt exists about the validity of both these earlier models. They presented a model based on an isotropic Heisenberg Hamiltonian involving more than one coupling constant, J. The extreme sensitivity of $\mu(T)$ to small changes in the ratio $J_2:J_1$ proved to be a serious problem. Without a larger range of model compounds the correlations between the chemical nature of the substituents on the Cu_4O tetrahedron and the magnetic behavior can be derived only with difficulties.

As part of a systematic study of the relationship between structure and magnetic behavior in tetranuclear μ_4-oxo-bridged copper(II) complexes, we have employed a new dinucleating ligand, 2,6-bis(morpholinomethyl)-4-methylphenol (Hbmmk).

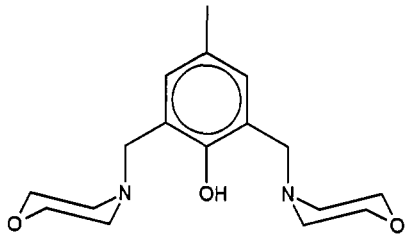

Hbmmk

Hbmmk was obtained by a Mannich reaction between a para-substituted phenol, formaldehyde, and morpholine. With this tridentate ligand we were able to prepare two tetramers of the new type $[Cu_4OX_4L_6]$, $[Cu_4OBr_4(bmmk)_2]\cdot 2MeOH$ (**1**) and $[Cu_4O(OBz)_4(bmmk)_2]\cdot H_2O$ (**2**). These μ_4-oxo-bridged cluster compounds are of particular interest because they are the first members of this class containing chelating ligands. This leads to significant perturbations in the $\{Cu_4O\}$ framework. In **1** one of the normally three halides in the basal plane of the trigonal bipyramidal arrangement around the copper ions is replaced by an oxygen atom. The coordination polyhedra show unusually strong distortions due to the sterical force of the chelating ligand. **2** is the first complex of this type in which all halide ions are replaced by benzoate groups. The copper centers are no longer trigonal bipyramidally coordinated. Two atoms show square pyramidal coordination; one is square planar, and for the fourth copper atom octahedral coordination can be observed. Nevertheless, a nearly perfect tetrahedron of four copper(II) atoms is observed around the central oxygen in **1**, and a slightly distorted tetrahedron in **2**. Besides the X-ray molecular structures of these two copper compounds, the magnetic and spectroscopic properties were studied in detail.

Experimental Section

All reagents were purchased from commercial sources and used as received. Solvents were dried by standard procedures prior to use. ^1H NMR spectra were recorded on a Bruker WH 300 instrument; all chemical shifts are reported in parts per million (ppm) relative to an internal standard of tetramethylsilane. Infrared spectra in the range 4000–200 cm^{-1} were recorded on a Perkin-Elmer 683 spectrophotometer using KBr as a diluting matrix. The FIR spectra (400–80 cm^{-1}) were recorded on a Bruker IF 113v instrument in a polyethylene matrix. All elemental analyses were performed at the Institute of Organic Chemistry, University of Münster.

Magnetic susceptibilities of powdered samples were recorded on a Faraday-type magnetometer using a sensitive Cahn RG electrobalance in the temperature range 4.2–475.4 K. The magnetic field applied was ≈1.2 T. Details of the apparatus have been described elsewhere.[10] Experimental susceptibility data were corrected for the underlying diamagnetism. Corrections for diamagnetism were estimated as -888×10^{-6} cm^3/mol and -918×10^{-6} cm^3/mol for complexes **1** and **2**, respectively.

Table 1. Crystallographic Data for the Complexes

	1	**2**
formula	$Cu_4C_{36}H_{58}N_4O_9Br_4$	$Cu_4C_{62}H_{72}N_4O_{16}$
fw	1264.68	1383.45
cryst dimens, mm	0.05 × 0.35 × 0.20	0.10 × 0.14 × 0.20
cryst syst	monoclinic	monoclinic
space group	$P2_1/c$	$P2_1$
a, Å	12.693(2)	11.889(2)
b, Å	12.378(2)	20.250(4)
c, Å	29.293(6)	12.481(3)
β, deg	96.32(3)	95.12(2)
V, Å^3	4574.4	2992.8
Z	4	2
T, K	150	293
ρ_{calcd}, g cm^{-3}	1.83	1.54
ρ_{obsd}, g cm^{-3} (293 K)	1.83	1.53
μ, cm^{-1}	5.38	1.48
transm factors: max, min	0.538, 0.131	0.711, 0.506
tot. no. of unique data	9920	6094
no. of data, $I > 2\sigma(I)$	5544	4792
no. of params refined	517	776
R (R_w)	0.032 (0.031)	0.087 (0.088)
goodness of fit	0.620	2.032

2,6-Bis(morpholinomethyl)-4-methylphenol (Hbmmk). The ligand was prepared according to literature methods.[11] Morpholine (11.7 mL, 135 mmol) was added to a solution of *p*-cresol (6.48 g, 60 mmol) in 30 mL of dioxane. The resulting mixture was stirred, and an aqueous solution of formaldehyde (11 mL of a 35% solution, 130 mmol) was slowly added. The solution was then heated to reflux and kept at this temperature for 2 h, after which the dioxane was evaporated under vacuum. The crude solid was recrystallized from toluene, yielding 4.68 g (26%) of Hbmmk. Mp: 118 °C. Anal. Calcd (found) for $C_{17}H_{26}N_2O_3$: C, 66.67 (67.20); H, 8.59 (8.80); N, 9.15 (9.04). ^1H NMR (acetone-d_6, δ): 2.19 (s, 3H), 2.46 (t, 8H), 2.80 (s, 1H), 3.56 (s, 4H), 3.63 (t, 8H), 6.89 (s, 2H) ppm.

$[Cu_4OBr_4(bmmk)_2]\cdot 2MeOH$ (1). Hbmmk (0.306 g, 1 mmol) was dissolved in 20 mL of methanol, and the solution was added to a 20-mL methanol solution of copper(II) bromide (0.447 g, 2 mmol). Upon standing at 25 °C, a dark brown crystalline solid deposited overnight and was collected by filtration, yielding 0.54 g (85%) of **1**. Anal. Calcd (found) for $Cu_4C_{36}H_{58}N_4O_9Br_4$: C, 34.16 (34.12); H, 4.59 (4.52); N, 4.43 (4.22).

$[Cu_4O(OBz)_4(bmmk)_2]\cdot H_2O$ (2). A 30-mL solution of Hbmmk (0.306 g, 1 mmol) in methanol was added to a solution of copper(II) perchlorate (0.740 g, 2 mmol) in 20 mL of methanol. A solution of sodium benzoate (0.720 g, 5 mmol) in 30 mL of methanol was added while stirring. The product was obtained by standing at room temperature as green crystals, which were collected by filtration, yielding 0.66 g (95%) of **2**. Anal. Calcd (found) for $Cu_4C_{62}H_{72}N_4O_{16}$: C, 53.38 (53.55); H, 5.21 (4.80); N, 4.01 (3.85).

X-ray Crystallography and Structure Determinations. Intensity data were collected on a Syntex $P2_1$ diffractometer (Mo Kα, λ = 0.710 73 Å, graphite monochromator) by using the ω-scan technique to maximum 2θ values of 54° (**1**) and 52° (**2**) and a variable scan rate (2–29°/min). The intensities of two reflections were monitored, and no significant crystal deterioration was observed. Further data collection parameters are summarized in Table 1.

The structures were solved by conventional Patterson and Fourier methods (**1**) or by direct methods (**2**). The remaining non-hydrogen atoms were located from a series of difference Fourier maps. Hydrogen atoms were included by using a riding model in which the coordinate shifts of the covalently bonded atoms were also applied to the hydrogen atoms (C–H distance held to 0.96 Å). Both structures were refined by full-matrix least-squares techniques using anisotropic thermal parameters for all non-hydrogen atoms in **1** and **2**. The isotropic thermal parameters for the hydrogen atoms were refined in groups for both structures: for

(8) Wong, H.; tom Dieck, H.; O'Connor, C. J.; Sinn, E. *J. Chem. Soc., Dalton Trans.* **1980**, 786–789.
(9) Jones, D. H.; Sams, J. R.; Thompson, R. C. *Inorg. Chem.* **1983**, *22*, 1399–1401.
(10) Merz, L.; Haase, W. *J. Chem. Soc., Dalton Trans.* **1980**, 875–879.
(11) Hodgkin, J. H. *Aust. J. Chem.* **1984**, *37*, 2371–2378.

Table 2. Final Positional and Isotropic Thermal Parameters (Å²) for **1**

atom	*x*	*y*	*z*	U_{eq}
Cu(1)	0.37115(5)	0.57868(5)	0.17229(2)	0.0135(2)
Cu(2)	0.13610(5)	0.60030(6)	0.14800(2)	0.0157(2)
Cu(3)	0.28164(5)	0.75747(5)	0.09830(2)	0.0165(2)
Cu(4)	0.27716(5)	0.52522(5)	0.06907(2)	0.0136(2)
Br(1)	0.48456(4)	0.72662(5)	0.14935(2)	0.0194(2)
Br(2)	0.37662(5)	0.39180(5)	0.11793(2)	0.0240(2)
Br(3)	0.15959(5)	0.82454(5)	0.15072(2)	0.0240(2)
Br(4)	0.05434(5)	0.54407(6)	0.07288(2)	0.0278(2)
C(1)	0.2209(4)	0.5284(5)	0.2432(2)	0.018(2)
C(2)	0.2979(4)	0.4665(5)	0.2689(2)	0.015(2)
C(3)	0.2798(5)	0.4334(5)	0.3133(2)	0.020(2)
C(4)	0.1885(5)	0.4593(5)	0.3321(2)	0.019(2)
C(5)	0.1718(5)	0.4288(6)	0.3805(2)	0.030(2)
C(6)	0.1119(5)	0.5198(5)	0.3051(2)	0.020(2)
C(7)	0.1272(4)	0.5563(5)	0.2612(2)	0.017(2)
C(8)	0.3954(4)	0.4316(5)	0.2481(2)	0.019(2)
C(9)	0.5628(4)	0.4803(5)	0.2181(2)	0.021(2)
C(10)	0.6364(5)	0.4525(6)	0.2610(2)	0.031(2)
C(11)	0.5554(5)	0.5834(6)	0.3036(2)	0.030(2)
C(12)	0.4790(4)	0.6131(5)	0.2621(2)	0.019(2)
C(13)	0.0465(4)	0.6265(5)	0.2333(2)	0.020(2)
C(14)	–0.0804(5)	0.6489(6)	0.1649(2)	0.028(2)
C(15)	–0.1824(5)	0.6220(7)	0.1845(2)	0.036(3)
C(16)	–0.1208(5)	0.4484(6)	0.2045(2)	0.033(2)
C(17)	–0.0180(5)	0.4695(6)	0.1848(2)	0.025(2)
C(18)	0.3124(4)	0.6992(4)	–0.0001(2)	0.015(2)
C(19)	0.3561(4)	0.7996(5)	–0.0085(2)	0.018(2)
C(20)	0.3685(5)	0.8282(5)	–0.0538(2)	0.024(2)
C(21)	0.3404(5)	0.7590(5)	–0.0903(2)	0.024(2)
C(22)	0.3548(6)	0.7899(6)	–0.1397(2)	0.034(2)
C(23)	0.2949(5)	0.6587(5)	–0.0810(2)	0.019(2)
C(24)	0.2788(4)	0.6293(5)	–0.0364(2)	0.017(2)
C(25)	0.3881(5)	0.8748(5)	0.0310(2)	0.023(2)
C(26)	0.3340(6)	0.9870(5)	0.0928(2)	0.029(2)
C(27)	0.3214(7)	1.0955(5)	0.0683(2)	0.039(3)
C(28)	0.1922(6)	1.0260(5)	0.0133(2)	0.031(2)
C(29)	0.1977(5)	0.9166(5)	0.0364(2)	0.026(2)
C(30)	0.2158(4)	0.5293(5)	–0.0280(2)	0.015(2)
C(31)	0.2053(5)	0.3517(5)	0.0081(2)	0.022(2)
C(32)	0.2111(6)	0.2814(5)	–0.0342(2)	0.030(2)
C(33)	0.3768(6)	0.3491(6)	–0.0454(2)	0.033(3)
C(34)	0.3783(5)	0.4223(5)	–0.0036(2)	0.022(2)
C(35)	0.1736(12)	0.2424(13)	0.1772(5)	0.064(5)
C(35A)	0.0701(15)	0.2206(16)	0.1800(6)	0.024(6)
C(36)	0.0183(13)	0.1295(14)	0.0894(6)	0.041(6)
C(36A)	0.0002(13)	0.1221(15)	0.0584(6)	0.049(6)
N(1)	0.4574(3)	0.5229(4)	0.2289(1)	0.016(2)
N(2)	0.0128(4)	0.5854(4)	0.1854(1)	0.020(2)
N(3)	0.3028(4)	0.8928(4)	0.0622(1)	0.021(2)
N(4)	0.2704(4)	0.4525(4)	0.0070(1)	0.014(2)
O(1)	0.2385(3)	0.5608(4)	0.2010(1)	0.020(1)
O(2)	0.6538(3)	0.5464(4)	0.2895(1)	0.034(2)
O(3)	–0.2051(3)	0.5085(5)	0.1803(1)	0.038(2)
O(4)	0.2684(3)	0.6147(3)	0.1220(1)	0.012(1)
O(5)	0.3004(3)	0.6691(3)	0.0432(1)	0.020(1)
O(6)	0.2145(4)	1.1090(4)	0.0469(1)	0.037(2)
O(7)	0.3175(4)	0.2529(4)	–0.0396(1)	0.038(2)
O(8)	0.1424(8)	0.1313(13)	0.1843(5)	0.182(7)
O(9)	–0.0377(10)	0.2155(12)	0.0711(6)	0.196(8)

1, $U_H(CH_3)$ = 0.07(1), $U_H(CH_2)$ = 0.022(3), $U_H(CH_{arom})$ = 0.017(7) Å²; for **2**; $U_H(CH_3)$ = 0.16(6), $U_H(CH_2)$ = 0.06(1) Å², $U_H(CH_{arom})$ = $1.3U_{C(bonded)}$. With exception of the disordered solvent molecules in **1** (*K*(C35A) = 0.66(2), *K*(C35B) = 0.34; *K*(C36A) = 0.51(4), *K*(C36B) = 0.49) the occupancy factors for all other atoms in **1** and **2** are *K* = 1. The function minimized was $\sum w(|F_o| - |F_c|)^2$, where $w = 1/[\sigma^2(F_o) + g(F_o)^2]$ and $g = 0.0001$, with final agreement factors of $R = \sum(||F_o| - |F_c||)/\sum|F_o|$ and $R_w = [\sum w(|F_o| - |F_c|)^2/\sum|F_o|^2]^{1/2}$. The highest peaks in the final difference Fourier maps were found to be 0.90 e/Å³ for **1** and 1.34 e/Å³ for **2**. All programs used were part of the Micro Vax version of the SHELXTL system of programs.[12] Final atomic coordinates and isotropic thermal parameters of compounds **1** and **2** are listed in Tables 2 and 3, respectively.

(12) Sheldrick, G. SHELXTL+. University of Göttingen, 1990.

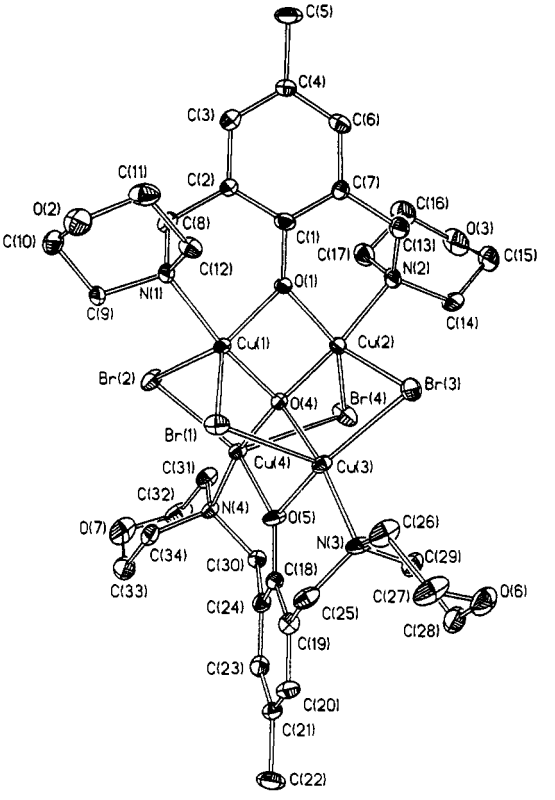

Figure 1. Molecular structure and atomic numbering scheme for the $[Cu_4OBr_4(bmmk)_2]$ complex in **1**. Hydrogen atoms are omitted for clarity. Ellipsoids are drawn at the 50% probability level.

Results and Discussion

Crystal and Molecular Structures. $[Cu_4OBr_4(bmmk)_2]$·2MeOH (1). Figure 1 illustrates the results of the X-ray study of **1** along with the labeling system used in the discussion. Selected interatomic distances, with their estimated standard deviations (esd's), are collected in Table 4; bond angles are given in Table 5.

The molecule consists of a tetrahedron of copper(II) atoms centered by a μ_4-bridging oxygen atom and with μ-bromine atoms bridging four of the six edges of the Cu_4 tetrahedron. The remaining two edges are occupied by μ-phenoxo bridges from the deprotonated bmmk⁻ ligand. The structure is completed by four terminal N-bonded morpholine groups, one of them per each copper atom. The tetrahedron around the central oxygen (O(4)) with Cu–O(4) distances of 1.909, 1.927, 1.913, and 1.919 Å for Cu(1)–Cu(4) (Table 4) shows unusually high distortion. The observed bond angles vary from 103.0 and 103.1° for Cu(1)–O(4)–Cu(2) and Cu(3)–O(4)–Cu(4) to 113.3 and 114.6° for Cu(2)–O(4)–Cu(4) and Cu(1)–O(4)–Cu(3) (Table 5). This distortion is caused by the steric force of the chelating ligands which contract each of the two copper centers within the tetranuclear unit (Cu(1), Cu(2) and Cu(3), Cu(4)), associated with a reduction of the corresponding Cu–O–Cu bond angles. Much less distortions are observed in the $\{Cu_4O\}$ frameworks of analogous complexes such as $Cu_4OCl_6(C_{11}H_{12}N_2)_4$,[5a] $Cu_4OCl_6(C_4H_6N_2)_4$,[5c] and $Cu_4OCl_6(OSMe_2)_4$,[5d] which include no chelating ligands. Nevertheless some distortion is observed in all reported examples that do not have crystallographically imposed symmetry. Guy et al.[5e] already noted that this distortion from the tetrahedral geometry to be a predominant feature for complexes of this type.

In analogy to the other structures reported from this series[5,6] the halide bridges also exhibit a large degree of asymmetry in their Cu–Br bond distances, which is quite interesting since all bromides are chemically equivalent and located in the basal planes of the coordination polyhedra around the copper centers. Each of the copper atoms is associated with one "long" (Cu(1)–Br(2)

Table 3. Final Positional and Isotropic Thermal Parameters (Å²) for **2**

atom	x	y	z	U_{eq}	atom	x	y	z	U_{eq}
Cu(1)	0.3591(2)	0.0467(1)	0.2606(2)	0.0279(6)	C(40)	0.770(2)	−0.090(2)	0.468(2)	0.068(9)
Cu(2)	0.2392(2)	−0.0620(1)	0.3655(2)	0.0304(7)	C(41)	0.691(2)	−0.070(1)	0.394(2)	0.056(8)
Cu(3)	0.3150(2)	−0.0941(1)	0.1318(2)	0.0306(7)	C(42)	0.120(2)	−0.162(1)	0.251(2)	0.038(7)
Cu(4)	0.1228(2)	0.0000	0.1473(2)	0.0289(7)	C(43)	0.007(1)	−0.194(1)	0.212(1)	0.035(6)
C(1)	0.430(1)	0.008(1)	0.485(1)	0.029(5)	C(44)	−0.093(2)	−0.170(1)	0.245(2)	0.037(6)
C(2)	0.451(1)	−0.047(1)	0.554(1)	0.032(6)	C(45)	−0.193(1)	−0.198(1)	0.206(1)	0.037(6)
C(3)	0.543(1)	−0.042(1)	0.632(1)	0.036(6)	C(46)	−0.196(2)	−0.248(1)	0.132(2)	0.051(8)
C(4)	0.611(1)	0.012(1)	0.643(2)	0.045(7)	C(47)	−0.099(2)	−0.273(1)	0.100(2)	0.059(9)
C(5)	0.708(2)	0.012(1)	0.727(2)	0.074(9)	C(48)	0.004(2)	−0.246(1)	0.139(2)	0.045(7)
C(6)	0.587(1)	0.065(1)	0.575(2)	0.043(7)	C(49)	0.302(1)	0.082(1)	0.038(2)	0.030(6)
C(7)	0.497(1)	0.065(1)	0.500(1)	0.030(5)	C(50)	0.345(2)	0.100(1)	−0.068(2)	0.035(6)
C(8)	0.377(1)	−0.106(1)	0.539(1)	0.025(5)	C(51)	0.451(2)	0.125(1)	−0.073(2)	0.045(7)
C(9)	0.219(2)	−0.047(1)	0.604(2)	0.042(7)	C(52)	0.485(2)	0.148(1)	−0.169(2)	0.071(10)
C(10)	0.089(2)	−0.040(1)	0.598(2)	0.077(10)	C(53)	0.416(3)	0.142(1)	−0.260(3)	0.076(12)
C(11)	0.073(2)	−0.153(1)	0.549(2)	0.065(9)	C(54)	0.314(3)	0.114(1)	−0.261(2)	0.069(10)
C(12)	0.200(2)	−0.160(1)	0.544(2)	0.054(8)	C(55)	0.272(2)	0.095(1)	−0.163(2)	0.056(8)
C(13)	0.462(1)	0.128(1)	0.436(1)	0.027(5)	C(56)	0.110(1)	0.088(1)	0.325(2)	0.034(6)
C(14)	0.417(2)	0.186(1)	0.270(2)	0.044(7)	C(57)	0.048(1)	0.113(1)	0.417(1)	0.029(5)
C(15)	0.492(2)	0.246(1)	0.291(2)	0.062(9)	C(58)	0.095(2)	0.157(1)	0.492(2)	0.070(10)
C(16)	0.650(1)	0.178(1)	0.304(2)	0.064(9)	C(59)	0.041(3)	0.179(1)	0.581(3)	0.090(12)
C(17)	0.581(1)	0.115(1)	0.285(2)	0.048(7)	C(60)	−0.066(2)	0.155(2)	0.589(3)	0.098(13)
C(18)	0.110(1)	−0.105(1)	−0.019(1)	0.032(6)	C(61)	−0.114(2)	0.116(2)	0.517(2)	0.085(12)
C(19)	0.004(2)	−0.083(1)	−0.061(1)	0.038(6)	C(62)	−0.061(2)	0.091(1)	0.427(2)	0.065(9)
C(20)	−0.069(2)	−0.124(1)	−0.117(2)	0.046(7)	N(1)	0.255(1)	−0.096(1)	0.523(1)	0.040(5)
C(21)	−0.036(2)	−0.190(1)	−0.15092)	0.053(8)	N(2)	0.462(1)	0.125(1)	0.317(1)	0.029(5)
C(22)	−0.117(2)	−0.235(1)	−0.210(2)	0.075(10)	N(3)	0.357(1)	−0.146(1)	−0.004(1)	0.035(5)
C(23)	0.072(2)	−0.207(1)	−0.117(2)	0.050(7)	N(4)	−0.032(1)	0.014(1)	0.064(1)	0.036(5)
C(24)	0.146(1)	−0.167(1)	−0.054(1)	0.034(6)	O(1)	0.346(1)	0.008(1)	0.407(1)	0.034(4)
C(25)	−0.026(1)	−0.009(1)	−0.050(2)	0.037(5)	O(2)	0.045(1)	−0.105(1)	0.624(1)	0.077(7)
C(26)	−0.122(1)	−0.020(1)	0.117(2)	0.046(7)	O(3)	0.601(1)	0.234(1)	0.251(1)	0.061(6)
C(27)	−0.238(2)	0.001(1)	0.078(2)	0.069(9)	O(4)	0.260(1)	−0.028(1)	0.224(1)	0.035(4)
C(28)	−0.177(2)	0.104(1)	0.019(2)	0.061(9)	O(5)	0.177(1)	−0.066(1)	0.043(1)	0.039(4)
C(29)	−0.056(1)	0.088(1)	0.063(2)	0.042(7)	O(6)	0.564(1)	−0.100(1)	−0.083(1)	0.057(5)
C(30)	0.261(2)	−0.195(1)	−0.021(2)	0.048(7)	O(7)	−0.253(1)	0.072(1)	0.088(2)	0.078(7)
C(31)	0.464(1)	−0.184(1)	0.010(2)	0.045(7)	O(8)	0.436(1)	−0.126(1)	0.234(1)	0.048(5)
C(32)	0.564(2)	−0.140(1)	0.011(2)	0.053(8)	O(9)	0.522(1)	−0.028(1)	0.237(1)	0.046(5)
C(33)	0.463(2)	−0.060(1)	−0.088(2)	0.050(7)	O(10)	0.112(1)	−0.115(1)	0.314(1)	0.057(6)
C(34)	0.360(2)	−0.104(1)	−0.099(2)	0.045(7)	O(11)	0.207(1)	−0.183(1)	0.218(1)	0.065(6)
C(35)	0.515(1)	−0.085(1)	0.274(2)	0.039(6)	O(12)	0.377(1)	0.071(1)	0.113(1)	0.035(4)
C(36)	0.600(2)	−0.110(1)	0.352(2)	0.041(7)	O(13)	0.199(1)	0.077(1)	0.047(1)	0.045(5)
C(37)	0.598(2)	−0.174(1)	0.399(2)	0.054(8)	O(14)	0.065(1)	0.039(1)	0.273(1)	0.046(5)
C(38)	0.679(2)	−0.193(1)	0.478(2)	0.077(10)	O(15)	0.202(1)	0.115(1)	0.309(1)	0.038(4)
C(39)	0.763(2)	−0.152(2)	0.515(2)	0.078(11)	O(16)	0.347(2)	0.737(1)	0.354(3)	0.148(13)

Table 4. Selected Interatomic Distances (Å) for **1**

Cu(1)–Br(1)	2.468(1)	Cu(1)–Br(2)	2.813(1)
Cu(1)–N(1)	2.006(4)	Cu(1)–O(1)	1.977(4)
Cu(1)–O(4)	1.909(3)	Cu(2)–Br(3)	2.792(1)
Cu(2)–Br(4)	2.429(1)	Cu(2)–N(2)	2.016(5)
Cu(2)–O(1)	1.974(3)	Cu(2)–O(4)	1.927(4)
Cu(3)–Br(1)	2.858(1)	Cu(3)–Br(3)	2.443(1)
Cu(3)–N(3)	2.016(5)	Cu(3)–O(4)	1.913(4)
Cu(3)–O(5)	1.985(4)	Cu(4)–Br(2)	2.444(1)
Cu(4)–Br(4)	2.852(1)	Cu(4)–N(4)	2.022(4)
Cu(4)–O(4)	1.919(3)	Cu(4)–O(5)	1.971(4)

Table 5. Selected Interatomic Angles (deg) for **1**

Br(1)–Cu(1)–Br(2)	113.9(1)	Br(1)–Cu(1)–N(1)	101.5(1)
Br(1)–Cu(1)–O(1)	138.5(1)	Br(1)–Cu(1)–O(4)	89.2(1)
Br(2)–Cu(1)–N(1)	98.0(1)	Br(2)–Cu(1)–O(1)	103.0(1)
Br(2)–Cu(1)–O(4)	79.2(1)	N(1)–Cu(1)–O(4)	169.1(2)
N(1)–Cu(1)–O(1)	91.3(2)	O(1)–Cu(1)–O(4)	79.2(1)
Br(3)–Cu(2)–Br(4)	110.1(1)	Br(3)–Cu(2)–N(2)	99.3(2)
Br(3)–Cu(2)–O(1)	99.5(1)	Br(3)–Cu(2)–O(4)	79.9(1)
Br(4)–Cu(2)–N(2)	100.8(1)	Br(4)–Cu(2)–O(1)	145.1(1)
Br(4)–Cu(2)–O(4)	88.4(1)	N(2)–Cu(2)–O(1)	91.9(2)
N(2)–Cu(2)–O(4)	170.4(1)	O(1)–Cu(2)–O(4)	78.9(1)
Br(1)–Cu(3)–Br(3)	108.3(1)	Br(1)–Cu(3)–N(3)	102.8(1)
Br(1)–Cu(3)–O(4)	78.3(1)	Br(1)–Cu(3)–O(5)	99.8(1)
Br(3)–Cu(3)–N(3)	100.2(1)	Br(3)–Cu(3)–O(4)	89.9(1)
Br(3)–Cu(3)–O(5)	147.0(1)	N(3)–Cu(3)–O(4)	168.7(2)
N(3)–Cu(3)–O(5)	89.8(2)	O(4)–Cu(3)–O(5)	79.0(1)
Br(2)–Cu(4)–Br(4)	118.9(1)	Br(2)–Cu(4)–N(4)	101.2(1)
Br(2)–Cu(4)–O(4)	89.4(1)	Br(2)–Cu(4)–O(5)	138.3(1)
Br(4)–Cu(4)–N(4)	97.3(1)	Br(4)–Cu(4)–O(4)	77.0(1)
Br(4)–Cu(4)–O(5)	97.6(1)	N(4)–Cu(4)–O(4)	169.4(2)
N(4)–Cu(4)–O(5)	92.9(2)	O(4)–Cu(4)–O(5)	79.2(1)
Cu(1)–Br(1)–Cu(3)	73.9(1)	Cu(1)–Br(2)–Cu(4)	74.5(1)
Cu(2)–Br(3)–Cu(3)	73.6(1)	Cu(2)–Br(4)–Cu(4)	74.5(1)
Cu(1)–O(4)–Cu(3)	114.6(2)	Cu(1)–O(4)–Cu(4)	113.1(2)
Cu(2)–O(4)–Cu(3)	110.1(2)	Cu(2)–O(4)–Cu(4)	113.3(2)
Cu(3)–O(4)–Cu(4)	103.1(1)	Cu(1)–O(4)–Cu(2)	103.0(1)

= 2.813 Å, Cu(2)–Br(3) = 2.792 Å, Cu(3)–Br(1) = 2.858 Å, Cu(4)–Br(4) = 2.852 Å) and one "short" (Cu(1)–Br(1) = 2.468 Å, Cu(2)–Br(4) = 2.429 Å, Cu(3)–Br(3) = 2.433 Å, Cu(4)–Br(2) = 2.444 Å) copper–bromine bond (Table 4).

The coordination of the four copper atoms is approximately trigonal bipyramidal. A nitrogen atom and the central μ_4-oxide occupy the axial positions, and two bromine and one phenolate ligands coordinate the equatorial sites. The copper atoms are displaced out of the planes of the equatorial ligand atoms by 0.285 Å (Cu(1)), 0.280 Å (Cu(2)), 0.274 Å (Cu(3)), and 0.299 Å (Cu(4)) in the direction of the nitrogen atoms of the morpholine groups. In agreement with the distortion by the chelating ligands there are two short copper–copper distances, Cu(1)···Cu(2) and Cu(3)···Cu(4) with 3.002(1) and 2.998(1) Å, respectively, and four long distances with 3.216(1), 3.195(1), 3.148(1), and 3.214(1) Å for Cu(1)···Cu(3), Cu(1)···C(4), Cu(2)···Cu(3), and Cu(2)···Cu(4). The N–Cu–Br angles range from 97.3 to 102.8° (average 100.1°) whereas the N–Cu–O_{eq} (eq = equatorial) angles are significantly smaller in the range from 89.8 to 92.9° (average 91.5°). The N–Cu–O_{ax} (ax = axial) angles vary from 168.7 to 170.4° (average 169.4°), and Br–Cu–Br angles range from 108.3 to 118.9° (average 112.8°). The Br–Cu–O_{eq} angles can be subdivided into two groups corresponding to the associated Cu–Br bond length.

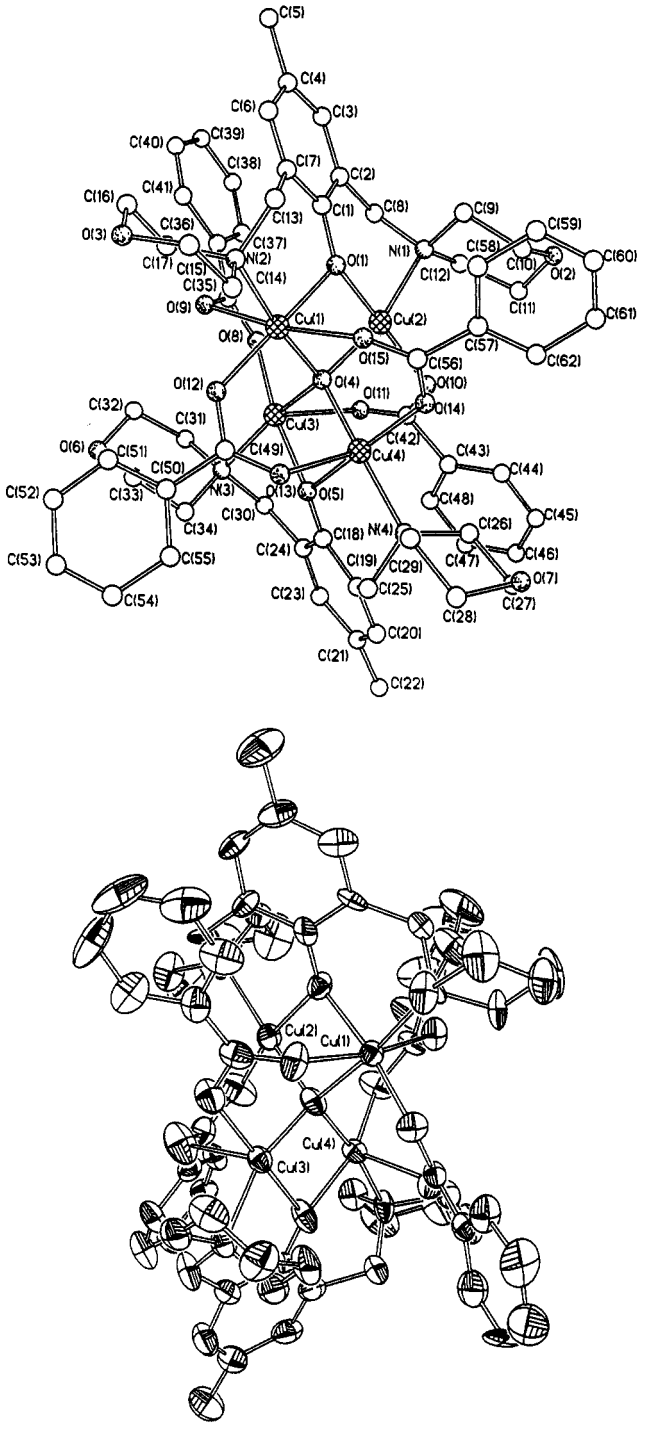

Figure 2. (a) Top: Molecular structure and atomic numbering scheme for the $[Cu_4O(OBz)_4(bmmk)_2]$ complex in **2**. Hydrogen atoms are omitted for clarity. (b) Bottom: Molecular geometry for $[Cu_4O(OBz)_4(bmmk)_2]\cdot H_2O$ (**2**). Hydrogens are omitted for clarity. Ellipsoids are drawn at the 50% probability level.

The Br–Cu–O_{eq} units with "long" Cu–Br bonds have smaller angles ranging from 97.6 to 102.8° (average 100.0°), whereas "short" Cu–Br bonds correspond to angles ranging from 138.5 to 147.0° (average 142.3°) (Table 5). The Cu–O and Cu–N bond lengths are, with an average of 1.945 and 2.011 Å, respectively, in the same range as in similar compounds. The unusually high axial distortion of the coordination polyhedra is due to the previously mentioned steric force by the chelating ligand. The observed distortions in the basal plane around the copper atoms are most likely to be van der Waals effects between the large bromine atoms and the remaining coordination framework.

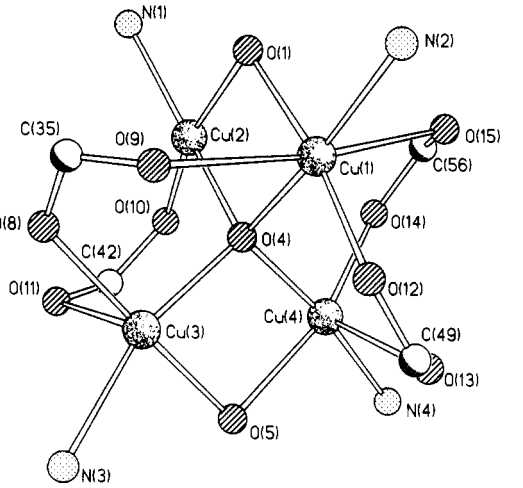

Figure 3. Inner coordination spheres of the copper atoms in $[Cu_4O(OBz)_4(bmmk)_2]\cdot H_2O$ (**2**).

Table 6. Selected Interatomic Distances (Å) for **2**

Cu(1)–N(2)	2.09(1)	Cu(1)–O(1)	2.00(1)
Cu(1)–O(4)	1.95(1)	Cu(1)–O(9)	2.49(1)
Cu(1)–O(12)	1.94(1)	Cu(1)–O(15)	2.44(1)
Cu(2)–N(1)	2.07(2)	Cu(2)–O(1)	1.94(1)
Cu(2)–O(4)	1.93(1)	Cu(2)–O(10)	1.92(1)
Cu(3)–N(3)	2.09(2)	Cu(3)–O(4)	1.92(1)
Cu(3)–O(5)	1.98(1)	Cu(3)–O(8)	1.94(1)
Cu(3)–O(11)	2.51(1)	Cu(4)–N(4)	2.05(1)
Cu(4)–O(4)	1.90(1)	Cu(4)–O(5)	2.02(1)
Cu(4)–O(13)	2.24(1)	Cu(4)–O(14)	1.93(1)

Finally, we note that the C–C, C–N, and C–O bond distances and angles in the ligand molecules are within their accepted range of values. The morpholine groups are present in their preferred chair conformation. A significant interaction between the molecules in the unit cell is not observed.

$[Cu_4O(OBz)_4(bmmk)_2]\cdot H_2O$ (2). The structural details of **2** are completely different from **1** although the main $\{Cu_4O\}$ framework is conserved. The geometry of **2** is shown in Figure 2a,b using the experimental atomic coordinates given in Table 3. Selected bond lengths and angles are given in Tables 6 and 7, respectively. In addition, Figure 3 enlarges the coordination unit of **2** to emphasize the exceptional geometry of this molecule.

The kernel of **2** is an oxygen atom surrounded tetrahedrally by four copper atoms. Two of these copper centers have a coordination geometry which approximates to square pyramidal; one is square planar, and one is octahedrally coordinated. This very unsymmetrical coordination of the metal centers is due to the nature of the $\mu_{1,3}$-benzoate bridge bonding which is described in detail below.

The copper tetrahedron around the μ_4-oxygen is even more distorted than in **1**. The bond distances vary from 1.90 Å for Cu(4)–O(4) and 1.92 Å for Cu(3)–O(4) to 1.93 Å for Cu(2)–O(4) and 1.95 Å for Cu(1)–O(4) (Table 6). The observed bond angles range from 100.7° for Cu(1)–O(4)–Cu(2) to 117.0° for Cu(1)–O(4)–Cu(3) (Table 7). Again this distortion can be explained by the steric forces of the chelating ligands which contract the Cu(1)–O(4)–Cu(2) and Cu(3)–O(4)–Cu(4) angles with a concomitant expansion of the other angles. The halide ions which normally μ-bridge the edges of the tetrahedron have been replaced by $\mu_{1,3}$-bridging benzoate groups. This leads to a significant loss of chemical symmetry because two benzoates are found to bridge the same tetrahedral edge between Cu(1) and Cu(4). Thereby one edge remains unbridged (Cu(2)–Cu(4)). The last two edges are again μ-phenoxo-bridged by the deprotonated ligand bmmk$^-$, in a fashion similar to that in compound **1**.

The arrangement of the ligands around the copper centers can be described as square basal planes with two further coordinating

Table 7. Selected Interatomic Angles (deg) for **2**

N(2)–Cu(1)–O(1)	94.6(5)	N(2)–Cu(1)–O(4)	173.8(6)
N(2)–Cu(1)–O(12)	90.9(5)	O(1)–Cu(1)–O(4)	79.4(5)
O(1)–Cu(1)–O(12)	171.7(5)	O(9)–Cu(1)–N(2)	93.5(5)
O(9)–Cu(1)–O(1)	89.8(5)	O(9)–Cu(1)–O(4)	87.8(5)
O(9)–Cu(1)–O(12)	83.8(5)	O(9)–Cu(1)–O(15)	172.4(6)
O(15)–Cu(1)–N(2)	85.7(5)	O(15)–Cu(1)–O(1)	82.7(5)
O(15)–Cu(1)–O(4)	92.2(5)	O(15)–Cu(1)–O(12)	103.8(5)
N(1)–Cu(2)–O(1)	89.2(5)	N(1)–Cu(2)–O(4)	167.2(5)
N(1)–Cu(2)–O(10)	98.0(6)	O(1)–Cu(2)–O(4)	81.2(5)
O(1)–Cu(2)–O(10)	166.8(5)	O(4)–Cu(2)–O(10)	93.1(6)
N(3)–Cu(3)–O(4)	162.7(5)	N(3)–Cu(3)–O(5)	86.2(5)
N(3)–Cu(3)–O(8)	98.7(6)	O(4)–Cu(3)–O(5)	80.1(5)
O(4)–Cu(3)–O(8)	96.3(5)	O(11)–Cu(3)–N(3)	99.0(5)
O(11)–Cu(3)–O(4)	91.7(5)	O(11)–Cu(3)–O(5)	90.7(5)
O(11)–Cu(3)–O(8)	81.9(5)	N(4)–Cu(4)–O(4)	170.7(5)
N(4)–Cu(4)–O(5)	94.9(5)	N(4)–Cu(4)–O(13)	90.3(5)
N(4)–Cu(4)–O(14)	89.4(5)	O(4)–Cu(4)–O(5)	79.6(5)
O(4)–Cu(4)–O(13)	96.7(5)	O(4)–Cu(4)–O(14)	93.7(5)
O(5)–Cu(4)–O(13)	86.3(5)	O(5)–Cu(4)–O(14)	161.9(5)
O(13)–Cu(4)–O(14)	111.3(5)		
Cu(1)–O(4)–Cu(2)	100.7(6)	Cu(1)–O(4)–Cu(3)	117.0(6)
Cu(1)–O(4)–Cu(4)	111.2(5)	Cu(2)–O(4)–Cu(3)	112.1(5)
Cu(2)–O(4)–Cu(4)	113.0(6)	Cu(3)–O(4)–Cu(4)	103.3(6)

oxygen atoms in axial positions at Cu(1) and one additional benzoate oxygen in the coordination spheres of Cu(3) and Cu(4). As can be expected, these further donating atoms in axial positions are less strongly bonded than the equatorial ligands, indicated by significantly longer bond distances. The copper atoms lie outside the plane defined by the four equatorial ligands. Cu(1) is displaced 0.048 Å to O(15), Cu(3) 0.018 Å to O(11) and Cu(4) 0.220 Å to O(13). Cu(2) is displaced by 0.031 Å out of the least-squares plane of its coordinating atoms. The basal plane angles around the copper ions fall into two sets which range from 79.4 to 98.7° (average 90.0°) and from 161.9 to 173.8° (average 168.3°) (Table 7). The large distortions of the trans angles as well as the bond angle distortions to the axially coordinated donors reflect the deviations of the copper atoms from the least-squares planes defined by the equatorial ligands. The average equatorial Cu–O bond length around Cu(2) (1.932 Å) is slightly smaller than the average bond length for the other copper ions (1.954 Å; Table 6). This may be an effect of the low coordination number of Cu(2), although the Cu–N bond lengths for Cu(1), Cu(3), and Cu(4) (average 2.074 Å) are in the same range as the Cu(2)–N bond length of 2.068 Å (Table 6). According to the expected Jahn–Teller distortion the bond distances to the axial benzoate donors are significantly longer with an average Cu–O distance of 2.422 Å.

Each of the bmmk$^-$ ligand molecules in **2** link two copper atoms (Cu(1), Cu(2) and Cu(3), Cu(4)) by a μ-phenoxo bridge. All morpholine-*N* and phenoxo donors are equatorially bonded, whereas the benzoate oxygens are coordinated alternatingly in axial and equatorial positions. As a result each benzoate is associated with one "short" and one "long" oxide–copper bond. This asymmetric bridge bonding is comparable to the known halide bridged structures similar to **1**; in the halide complexes, however, the electronic reason for this asymmetry is not quite clear.

Again two short (Cu(1)···Cu(2) = 2.988(3) Å, Cu(3)···Cu(4) = 2.995(3) Å) and four long (Cu(1)···Cu(3) = 3.293(3) Å, Cu(1)···Cu(4) = 3.175(3) Å, Cu(2)···Cu(3) = 3.196(3) Å, Cu(2)···Cu(4) = 3.199(3) Å) copper–copper distances are observed in the structure of **2**. All bond angles and distances within the ligand molecules are within their accepted range of values.

Magnetic Properties. Magnetic susceptibility data for solid samples of **1** and **2** were collected in the temperature range 4.2–475.4 K. The data are summarized in Table 8 and displayed in Figures 4 and 5 as μ_{eff} and molar susceptibility vs temperature.

The complexes **1** and **2** are characterized by having low room-temperature magnetic moments [**1**, μ_{eff} = 0.93 μ_B (294.6 K); **2**, μ_{eff} = 1.24 μ_B (298.5 K)], indicating significant antiferromagnetic coupling between the copper (II) centers; i.e., the data show clearly that the complexes possess a S = 0 ground state.

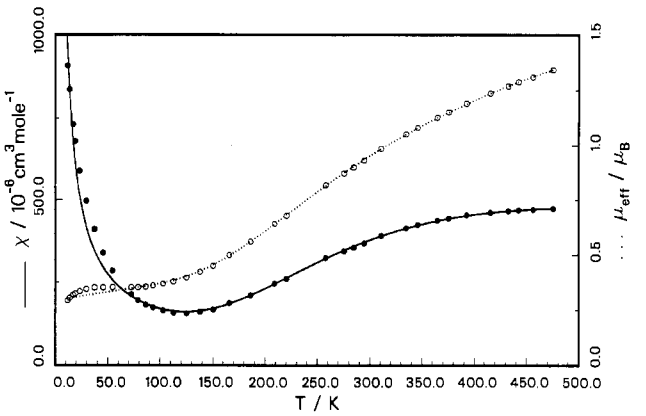

Figure 4. Variation of the experimental data for χ (●) and μ_{eff} (○) with temperature and calculated values for χ (—) and μ_{eff} (···) for $[Cu_4OBr_4(bmmk)_2]\cdot 2MeOH$ (**1**).

Table 8. Experimental and Calculated Magnetic Susceptibility Data for **1** and **2**

complex **1**				complex **2**			
T, K	χ_{exptl}	χ_{calc} (eq 6)	χ_{calc} (eq 2)	T, K	χ_{exptl}	χ_{calc} (eq 6)	χ_{calc} (eq 2)
11.8	906.9	968.4	967.6	7.0	452.8	477.2	477.3
13.8	835.9	836.8	836.0	10.2	343.6	346.3	346.4
17.2	731.5	683.2	682.6	12.0	303.5	303.4	303.4
19.2	679.6	618.3	617.8	12.9	287.4	286.4	286.4
23.7	588.1	512.3	511.9	15.0	247.2	254.7	254.7
29.9	496.2	418.5	418.2	17.0	245.0	231.8	231.8
37.5	410.3	345.8	345.6	19.4	218.3	210.5	210.6
45.5	338.8	295.6	295.4	25.4	179.9	175.0	175.0
54.5	284.7	256.7	256.5	34.0	142.5	145.9	145.9
72.5	213.6	208.0	207.9	38.1	130.3	136.7	136.7
79.0	195.8	196.1	196.0	45.8	119.1	124.3	124.3
86.3	182.1	185.2	185.1	56.5	108.9	115.3	115.3
93.2	173.7	177.0	176.9	63.0	108.9	114.4	114.5
103.0	164.5	168.4	168.3	68.5	112.8	116.6	116.8
112.9	157.6	163.0	163.0	71.9	116.6	119.5	119.7
125.2	155.7	160.9	160.9	79.2	130.9	129.5	129.7
138.1	160.5	163.8	163.8	86.6	148.9	144.8	145.2
150.4	167.5	170.9	171.0	92.9	166.8	161.7	162.1
165.8	187.0	185.0	185.1	103.2	202.8	195.8	196.2
186.2	210.5	210.5	210.5	113.2	242.4	234.5	234.9
209.0	245.8	244.7	244.6	125.2	287.5	285.1	285.3
220.5	260.6	263.0	262.8	138.2	340.9	340.9	340.9
258.0	323.4	321.2	321.2	149.5	382.3	387.7	387.5
275.5	344.2	346.6		165.2	435.4	447.1	446.7
284.5	355.2	358.6		185.3	496.0	510.7	510.2
294.6	367.7	371.2		208.8	550.1	566.6	566.1
310.7	390.9	389.7		216.5	562.9	580.8	580.3
334.6	413.7	413.1		238.0	602.8	611.5	611.1
345.7	423.8	422.4		254.2	620.7	627.0	626.8
364.6	437.2	436.1		272.0	633.0	638.0	637.9
375.4	443.8	442.8		282.0	637.3	642.0	641.9
392.4	453.5	454.8		298.5	645.6	645.5	645.5
415.5	461.4	461.2		313.7	646.9	646.0	646.1
432.5	466.2	466.4		334.6	644.1	643.6	643.7
442.4	468.7	468.8		346.7	642.7	640.8	640.9
456.3	470.1	471.5		360.6	639.8	636.7	636.8
475.4	473.6	474.1		374.7	637.8	631.7	631.8
				391.6	624.0	624.8	624.9
				414.6	615.0	614.4	614.5
				432.6	606.0	605.8	605.8
				443.6	600.2	600.2	600.2
				457.6	593.0	593.0	593.0
				475.4	584.0	583.9	583.8

Three different exchange pathways can occur in complexes **1** and **2**: $Cu–O_{Phenolate}–Cu$, $Cu–O_{oxo}–Cu$, and Cu–X–Cu (X = Br in **1** and OBz in **2**). Regarding the relatively large average Cu–

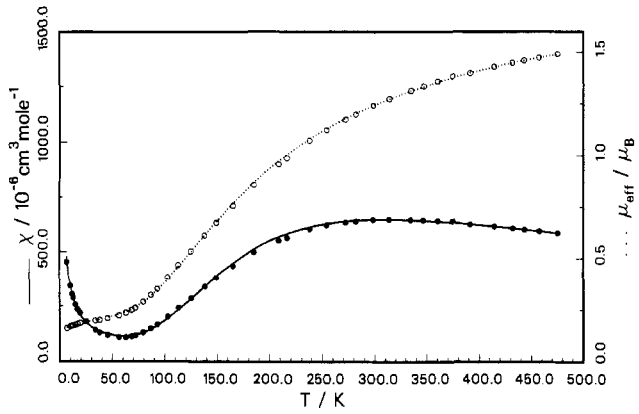

Figure 5. Variation of the experimental data for χ (●) and μ_{eff} (○) with temperature and calculated values for χ (—) and μ_{eff} (···) for $[Cu_4O(OBz)_4(bmmk)_2]\cdot H_2O$ (**2**).

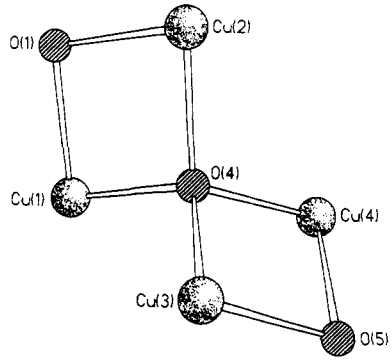

Figure 6. Connection of the Cu_2O_2 rings in **1** and **2**.

Br distances in **1** and the well-known magneto–structural correlations for equivalent Cu–Br–Cu systems,[13] a significant contribution of the Cu–Br–Cu pathway in **1** can be excluded. It was found that for (μ-carboxylato)copper(II) systems, only those compounds which exhibit an approximately square planar copper coordination show a strong contribution of the carboxylato ligand to the overall exchange.[14–16] Hence, the effect of the Cu–OBz–Cu pathways in **2** is also negligible. Investigations of copper(II) dimers confirm[17] that the Cu–O–Cu pathways should dominate and cause strong antiferromagnetic coupling. The effect of other bridging ligands such as Br^- in **1** or OBz^- in **2** should only slightly modulate the extent of coupling.

To explain the magnetic behavior of complexes **1** and **2**, their structures can consequently be reduced to a central Cu_4O_3 core which can be described as two O(4)-connected Cu_2O_2 rings as shown in Figure 6. The Cu–Br–Cu and Cu–OBz–Cu pathways in **1** and **2**, respectively, are assumed to have only a second-order effect upon the magnetic exchange between the copper centers. The tetranuclear copper(II) complex can be formally divided into two dinuclear Cu_2O_2 subunits. The intradimer coupling via two oxygen atoms is assumed to be larger than the interdimer exchange interactions via the O(4)-oxygen atom. Hence initially a molecular field model[18] was used to approximate the case where interdimer magnetic coupling (i.e. the exchange between the di-μ-oxo-bridged copper centers) is expected to dominate the relatively weaker interdimer coupling.

(13) For a review see: Willett, R. D. In *Magneto-Structural Correlations in Exchange Coupled Systems*; Willett, R. D., Gatteschi, D., Kahn, O., Eds.; D. Reidel Publishing Co.: Dordrecht, The Netherlands, 1985; pp 389–420 (see also references therein).
(14) Butcher, R. J.; Diven, G.; Erickson, G.; Mockler, G. M.; Sinn, E. *Inorg. Chim. Acta* **1986**, *123*, L17–L19.
(15) Berends, H. P.; Stephan, D. W. *Inorg. Chim. Acta* **1985**, *99*, L53–L59.
(16) Sorrell, T. N.; O'Connor, C. J.; Anderson, O. P.; Reibenspies, H. *J. Am. Chem. Soc.* **1985**, *107*, 4199–4206.
(17) Karlin, K. D.; Farooq, A.; Hayes, J. C.; Cohen, B. I.; Rowe, T. M.; Sinn, E.; Zubieta, J. *Inorg. Chem.* **1987**, *26*, 1271–1280.
(18) O'Connor, C. J. *Prog. Inorg. Chem.* **1982**, *29*, 203–283.

The experimental data may be analyzed under a first approximation by using a simple model for dinuclear compounds (eq 1), corrected for a weak interaction to compensate for the presence

$$\chi' = \frac{Ng^2\mu^2}{kT}\frac{\exp(-J/kT)}{1 + 3\exp(-J/kT)} \quad (1)$$

$$\chi = (1 - x_p)\frac{\chi'}{1 - (2z'J'/Ng^2\mu^2)\chi'} + x_p\frac{Ng^2\mu^2}{3kT}S(S+1) + \text{TIP} \quad (2)$$

of a tetranuclear molecule as shown in eq 2. A correction for a small amount (x_P) of paramagnetic impurity ($S = {}^1/_2$) was also taken into account. The last term represents the temperature-independent paramagnetism (TIP, 60×10^{-6} cm^3/mol for each copper atom). The best fit parameters are $g = 2.19$, $J = -296$ cm^{-1}, $z'J' = -33.4$ cm^{-1}, and $x_P = 2.4\%$ for **1** and $g = 2.00$, $J = -174$ cm^{-1}, $z'J' = -16.5$ cm^{-1}, and $x_P = 0.7\%$ for **2**. Fitting of the magnetic data to this modified Bleaney–Bowers expression for a copper dimer was only successful if a relatively large interdimer constant $z'J'$ was employed. This clearly indicates the presence of a significant interdimer coupling. The molecular field approximation fails if the magnitude is at least 5–10 times the magnitude of $z'J'$.

The data were consequently fitted to a more accurate model. The spin Hamiltonian for complexes **1** and **2**, assuming interaction in each pair can be properly described in terms of the Heisenberg Hamiltonian of the form $H = -2J_{ij}S_i\cdot S_j$, is given in eq 3. There

$$H = -2[J_{12}S_1\cdot S_2 + J_{13}S_1\cdot S_3 + J_{14}S_1\cdot S_4 + J_{23}S_2\cdot S_3 + J_{24}S_2\cdot S_4 + J_{34}S_3\cdot S_4] \quad (3)$$

is a maximum of six different exchange constants in a tetranuclear complex according to six different Cu–Cu dimeric units which can be taken into account. Due to the presence of only two types of bridging ligands, these are reduced to only two different exchange coupling constants. For an arrangement of copper(II) ions as shown in Figure 6, eq 3 degenerates directly to eq 4. With

$$H = -2[J_{12}(S_1\cdot S_2 + S_3\cdot S_4) + J_{13}(S_1\cdot S_3 + S_1\cdot S_4 + S_2\cdot S_3 + S_2\cdot S_4)] \quad (4)$$

$S_A = S_1 + S_2$, $S_B = S_3 + S_4$, $S_T = S_A + S_B$, and $S = {}^1/_2$, specifying S_T, S_A, S_B, and S uniquely defines an eigenstate of the Hamiltonian which will be represented by the notation $|S_T,S_A,S_B\rangle$ and which has the energy given by eq 5. The susceptibility can be expressed

$$E(S_T,S_A,S_B) = -J_{12}[S_A(S_A+1) + S_B(S_B+1) - 4S(S+1)] + -J_{13}[S_T(S_T+1) - S_A(S_A+1) - S_B(S_B+1)] \quad (5)$$

theoretically by eq 6, with $x = J_{12}/kT$ and $y = J_{13}/kT$. The best

$$\chi_{Cu_4} = (1 - x_p)\frac{Ng^2\mu^2}{kT}\{[10\exp(2x) + 2\exp(-2x) + 4\exp(-2y)]/[5\exp(2x) + 3\exp(-2x) + \exp(-4x) + 6\exp(-2y) + \exp(-4y)]\} + \exp\left(\frac{Ng^2\mu^2}{3kT}\right)S(S+1) + \text{TIP} \quad (6)$$

parameters which were obtained using a standard least-squares fitting program were $g = 2.19$, $J_{12} = -296$ cm^{-1}, $J_{13} = -36$ cm^{-1}, and $x_P = 2.4\%$ for complex **1** and $g = 2.01$, $J_{12} = -175$ cm^{-1}, $J_{13} = -18$ cm^{-1}, and $x_P = 0.8\%$ for complex **2**. The susceptibility data consistent with this set were found to be relatively insensitive to J_{13} but very sensitive to J_{12}. If the J_{12} interaction is strongly antiferromagnetic, a variation in J_{13} shows only in the higher

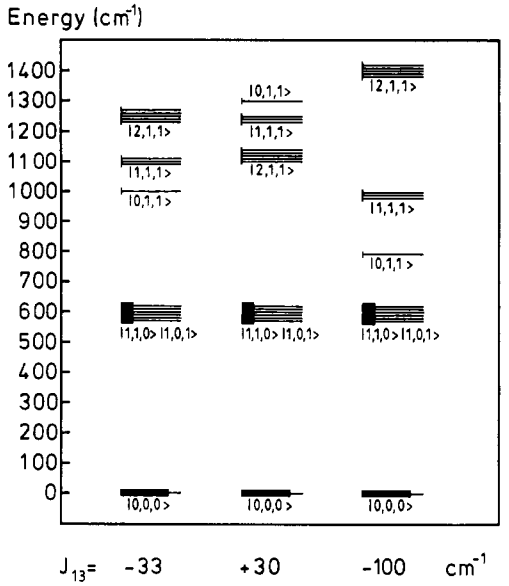

Figure 7. Relative energy levels of complex **1** for $J_{12} = -295$ cm^{-1} and $J_{13} = -33$, +30, and −100 cm^{-1} at 300 K.

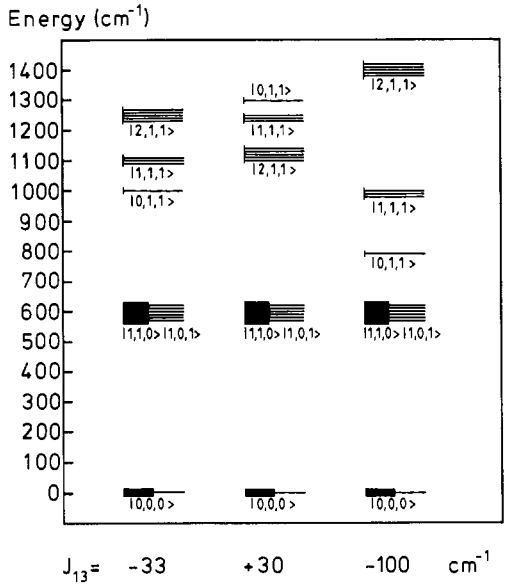

Figure 8. Relative energy levels of complex **1** for $J_{12} = -295$ cm^{-1} and $J_{13} = -33$, +30, and −100 cm^{-1} at 500 K.

magnetic states, not in the states that are thermally populated at 300 K. The data up to 300 K were not sufficient to discriminate and establish an accurate value of J_{13}. Therefore, susceptibility data were measured at higher temperatures up to 475 K. At 300 K none of the higher excited states contribute significantly to the magnetic susceptibilies of **1** and **2**. This is illustrated in Figures 7 and 8, which show the relative energy levels and their populations in the case of complex **1** for $J_{12} = -295$ cm^{-1} and $J_{13} = -33$, +30, and −100 cm^{-1} at 300 and 500 K.

Gorun and Lippard[19] have shown that in the case of iron(III) centers bridged by a ligand oxygen atom (oxo, hydroxo, alkoxo, etc.) the quantitative magneto–structural relationships which have been found for dinuclear complexes can also be applied to polynuclear iron clusters. Due to the decomposition of the tetranuclear complexes in two dimeric subunits, the different magnetic behaviors of **1** and **2** can also be explained by means of magneto–structural correlations. For symmetrical oxygen-bridged copper(II) compounds, a rather significant linear relationship has been found between magnetic exchange coupling

(19) Gorun, S. M.; Lippard, S. J. *Inorg. Chem.* **1991**, *30*, 1625–1630.

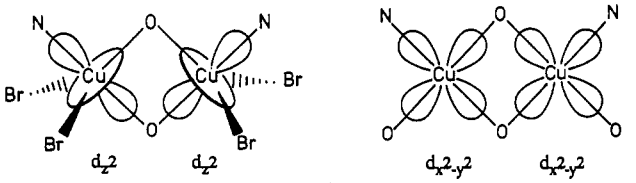

Figure 9. Schematic representation of the orbital orientations in $[Cu_4OBr_4(bmmk)_2]\cdot 2MeOH$ (**1**) (left) and $[Cu_4O(OBz)_4(bmmk)_2]\cdot H_2O$ (**2**) (right).

and the Cu–O–Cu angle.[13,20] The exchange interaction for bis(μ-hydroxo)copper(II) complexes should be ferromagnetic for Cu–O–Cu angles less than 97.5°. An opening of the Cu–O–Cu angle is connected with a transition from ferromagnetic to antiferromagnetic coupling. For di-μ-alkoxo compounds a similar correlation exists. Unsymmetrically μ-phenoxo-bridged copper(II) complexes with exchangeable exogenic ligands (average 2.074 Å) exhibit a reasonable linear dependence of the exchange integral on the average bridging angle.[21] It should be emphasized that the asymmetry of the dinuclear copper compounds due to different bridging ligands and angles does not lead to considerable deviations from known magneto–structural correlations for similar symmetrically bridged copper(II) dimers.

The average Cu–O–Cu angles in the Cu_2O_2 rings of **1** and **2** are 101.4 and 99.9°, respectively. Melnik[20] found that in the case of bis(μ-hydroxo)-bridged copper(II) complexes an increase of 1.5° in the Cu–O–Cu angle is associated with an increase in antiferromagnetic coupling of $\approx$80 cm^{-1}. For unsymmetrically bridged copper(II) complexes, a similar correlation was obtained.[21] Hence, the different values of J_{12} in **1** and **2** can be explained in terms of these magneto–structural correlations.

On the basis of the above results, we suggest that for the complexes which can be magnetically divided into Cu_2O_2 subunits, exchange coupling interactions will also follow the magneto–structural relationships described above.

Spectroscopic Results. In the infrared powder spectra of both tetranuclear complexes the characteristic bands of the organic ligand bmmk$^-$ are the most prominent features. Coordination through the morpholine nitrogen results in a decrease of the N–C stretching frequency of this group. For **2** the IR absorption of the carboxylate ions at 1600 cm^{-1} and the characteristic absorptions for the monosubstituted benzoate group at 720 and 680 cm^{-1} are observed. In addition both complexes exhibit strong IR absorptions at 592 and 581 cm^{-1} for **1** and **2**, respectively, which can be associated with ν(Cu–O) frequencies originating from vibrations in the Cu_4O core.[4b,22] We find a broad, medium-intensity band at ca. 520 cm^{-1} which we assign to ν(Cu–O) vibrations for bonds to the phenolate and carboxylate groups. No significant band down to energies of 100 cm^{-1} was found which could be assigned to ν(Cu–Br) frequencies. Comparison of the infrared spectrum of the copper(II) bromide cluster with the spectrum of the analogous tetramer, $[Cu_4OCl_4(bmmk)_2]$,[23] showed the spectra to be essentially identical, except that for the chloride analog we find an intense band at 224 cm^{-1} which we assign to ν(Cu–Cl). The apparent shift to lower energy for **1** is consistent with vibrational differences between metal–chlorine and metal–bromine bonds.

The electronic absorption spectra for complexes **1** and **2** in methanol solutions show distinct maxima between 240 and 730 nm. Transitions below 300 nm are assigned to ligand $\pi \rightarrow \pi^*$ transitions of the Hbmmk ligand, which occur at 287 nm (ϵ = 9670 M^{-1} cm^{-1}) for the free ligand. The spectra of the complexes show a transition around 290 nm also (**1**, λ_{max} = 292 nm, ϵ =

(20) Melnik, M. *Coord. Chem. Rev.* **1982**, *42*, 259–388.
(21) Lorösch, J.; Quotschalla, U.; Haase, W. *Inorg. Chim. Acta* **1987**, *131*, 229–236.
(22) tom Dieck, H.; Brehm, H.-P. *Chem. Ber.* **1969**, *102*, 3577–3583.
(23) Teipel, S.; Krebs, B. Unpublished results.

11 100 M^{-1} cm^{-1}; **2**, λ_{max} = 292 nm, ϵ = 14 800 M^{-1} cm^{-1}), but those peaks are stronger than the one for the free ligand. We expect that the 292-nm peak observed for the complexes to be predominant due to morpholine-N → copper(II) charge-transfer transitions. Complex **1** exhibits a phenolate → Cu(II) CT band at 337 nm (ϵ = 3550 M^{-1} cm^{-1}) and a broad band at 730 nm (ϵ = 112 M^{-1} cm^{-1}), assigned as the sum of the three possible d–d transitions. These transitions shift to 342 nm (ϵ = 7030 M^{-1} cm^{-1}) and 675 nm (ϵ = 298 M^{-1} cm^{-1}) for complex **2**, where benzoate groups have replaced the bromide ions. The increase and shift of the oxygen → Cu(II) CT band can be explained by an overlap of the phenolate and carboxylate → copper(II) charge-transfer bands in this complex.

The large shift in the position of the d–d transition to higher energies as compared to the one of complex **1** results from an increased overlap of the bridging phenolate p orbitals with the copper $d_{x^2-y^2}$ orbitals in **2**.[24] The geometries around the copper(II) ions in complex **2** are essentially square planar with additionally bonded benzoate oxygen atoms in axial positions. This results from the different orbital orientations as compared to complex **1** (Figure 9).

Acknowledgment. This research was supported by the Bundesminister für Forschung und Technologie and by the Deutsche Forschungsgemeinschaft. Financial support by the Fonds der Chemischen Industrie is gratefully acknowledged.

Supplementary Material Available: Figures showing unit cells and listings of hydrogen atom coordinates, anisotropic temperature factor coefficients, and additional interatomic distances and angles (15 pages). Ordering information is given on any current masthead page.

(24) (a) Maloney, J. J.; Glogowski, M.; Rohrbach, D. F.; Urbach, F. L. *Inorg. Chim. Acta* **1987**, *127*, L33–L35. (b) Oberhausen, K. J.; Richardson, J. F.; Buchanan, R. M.; McCusker, J. K.; Hendrickson, D. N.; Latour, J.-M. *Inorg. Chem.* **1991**, *30*, 1357–1365.